

Electronic Supplementary Information

Mono-, di- and tri-nuclear Pt^{II}(C[^]N)(N-donor ligand)Cl complexes showing aggregation-induced phosphorescent emission (AIPE) behavior for efficient solution-processed organic light-emitting devices †

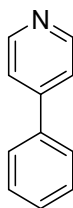
Xi Chen,^a Yuling Sun,^a Xinyi Zhao,^a Xuming Deng,^a Xiaolong Yang,^a Yuanhui Sun,^a
Guijiang Zhou*^a and Zhaoxin Wu^b

^aSchool of Chemistry, MOE Key Laboratory for Nonequilibrium Synthesis and Modulation of Condensed Matter, Xi'an Jiaotong University, Xi'an 710049, People's Republic of China. E-mail: zhougj@mail.xjtu.edu.cn

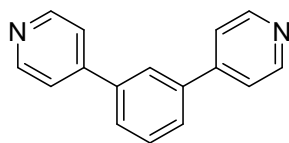
^bKey Laboratory of Photonics Technology for Information, School of Electronic and Information Engineering, Xi'an Jiaotong University, Xi'an 710049, People's Republic of China. E-mail: zhaoxinwu@mail.xjtu.edu.cn

Contents

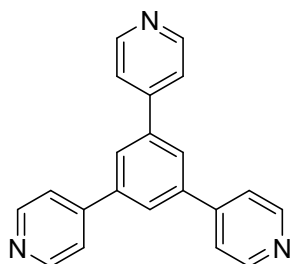
Synthesis of the key intermediate compounds	S3
Fig. S1 ¹ H NMR spectrum and ¹³ C NMR spectrum of Ph-PAYPt1	S6
Fig. S2 ¹ H NMR spectrum and ¹³ C NMR spectrum of Ph-PAYPt2	S7
Fig. S3 ¹ H NMR spectrum and ¹³ C NMR spectrum of Ph-PAYPt3	S8
Fig. S4. PL spectra of these mono-, di- and tri-nuclear Pt ^{II} (C [^] N)(N-donor ligand)Cl complexes in CH ₂ Cl ₂ at 77 K.	S9
Fig. S5 CV curves for Ph-PAYPt1 , PhPAYPt2 and PhPAYPt3	S9
OLED fabrication and measurements	S10
Fig. S6. EL spectrum for the devices except the optimized ones.	S11
Fig. S7. Current density–voltage–luminance (<i>J–V–L</i>) curves for the devices except the optimized ones.	S12
Fig. S8. Relationship between EL efficiencies and luminance for the devices except the optimized ones. (a) Device A1 , (b) Device A3 , (c) Device B1 , (d) Device B3 , (e) Device C1 and (f) Device C3 .	S13

Ph-N1

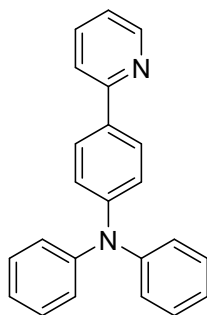
Under a nitrogen atmosphere, bromobenzene (5.00 g, 0.03 mol), pyridyl-4-boronic acid (4.70 g, 0.04 mol) and Pd(PPh₃)₄ (1.84 g, 1.59 mmol) were heated to 110 °C for 16 h in the mixture of 1,4-dioxane (20 mL) and Na₂CO₃ (2 M, 10 mL) under vigorous stirring. After the reaction, the mixture was extracted with CH₂Cl₂ and then purified by column chromatography, using CH₂Cl₂ and ethyl acetate as the eluent. The products were obtained as white solid (4.29 g, 87%). ¹H NMR (400 MHz, CDCl₃): δ (ppm) 8.66 (d, *J* = 6.0 Hz, 2H), 7.66-7.63 (m, 2H), 7.52-7.44 (m, 5H); FAB-MS (*m/z*): 155 [M]⁺; Anal. Calcd for C₁₁H₉N: C 85.13, H 5.85, N 9.03; found, C 85.04, H 5.76, N 8.96.

Ph-N2

Under a nitrogen atmosphere, 1,3-dibromobenzene (5.00g, 0.02 mol), pyridyl-4-boronic acid (6.26 g, 0.05 mol) and Pd(PPh₃)₄ (1.22 g, 1.06 mmol) were heated to 110 °C for 16 h in the mixture of 1,4-dioxane (20 mL) and Na₂CO₃ (2 M, 10 mL) under vigorous stirring. After the reaction, the mixture was extracted with CH₂Cl₂ and then purified by column chromatography, using CH₂Cl₂ and ethyl acetate as the eluent. The products were obtained as white solid (3.69 g, 75%). ¹H NMR (400 MHz, CDCl₃): δ (ppm) 8.70 (d, *J* = 4.0 Hz, 4H), 7.86 (s, 1H), 7.71-7.69 (m, 2H), 7.63-7.59 (m, 2H), 7.50 (d, *J* = 6.0 Hz, 4H); FAB-MS (*m/z*): 232 [M]⁺; Anal. Calcd for C₁₆H₁₂N₂: C 82.73, H 5.21, N 12.06; found, C 82.65, H 5.16, N 11.98.

Ph-N3

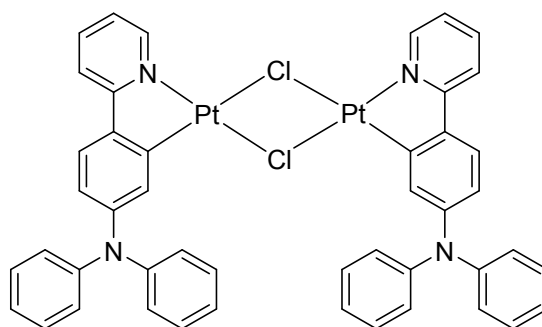
Under a nitrogen atmosphere, 1,3,5-tribromobenzene (5.00 g, 0.02 mol), pyridyl-4-boronic acid (7.03 g, 0.06 mol) and Pd(PPh₃)₄ (0.92 g, 0.79 mmol) were heated to 110 °C for 16 h in the mixture of 1,4-dioxane (20 mL) and Na₂CO₃ (2 M, 10 mL) under vigorous stirring. After the reaction, the mixture was extracted with CH₂Cl₂ and then purified by column chromatography, using CH₂Cl₂ and ethyl acetate as the eluent. The products were obtained as white solid (3.14 g, 64%). ¹H NMR (400 MHz, CDCl₃): δ (ppm) 8.75 (d, *J* = 5.2 Hz, 6H), 7.92 (s, 3H), 7.61 (d, *J* = 6.0 Hz, 6H); FAB-MS (*m/z*): 309 [M]⁺; Anal. Calcd for C₂₁H₁₅N₃: C 81.53, H 4.89, N 13.58; found, C 81.45, H 4.80, N 13.46.

L-N

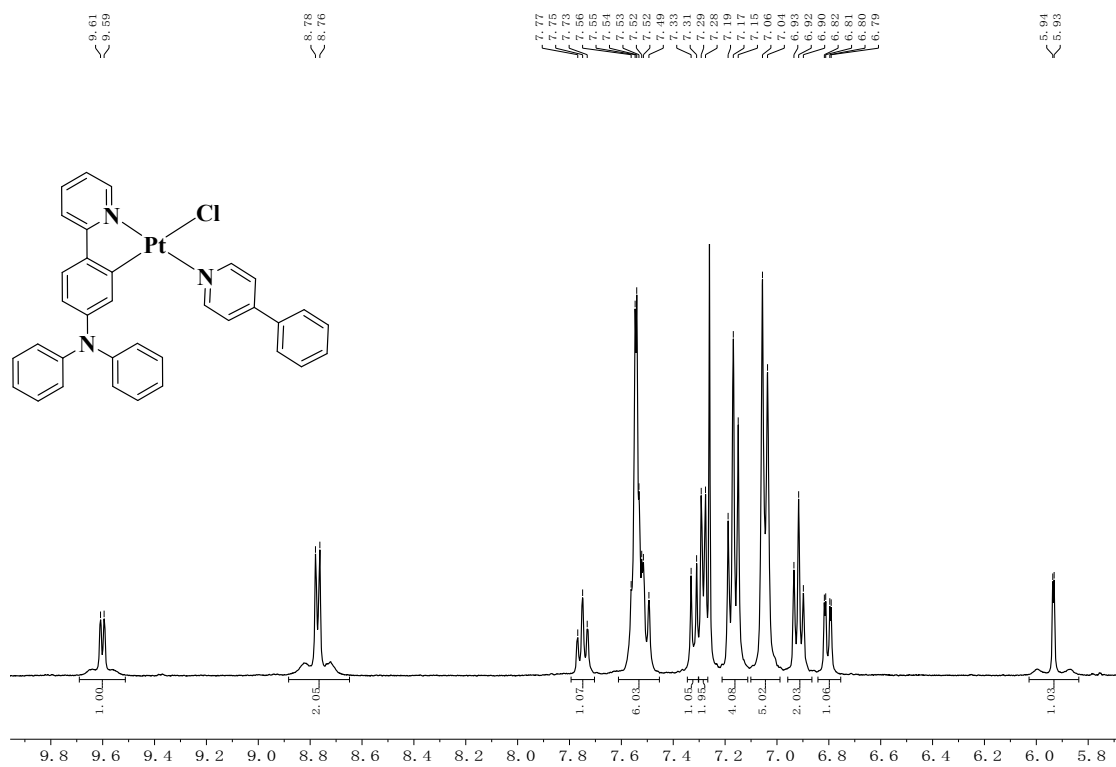
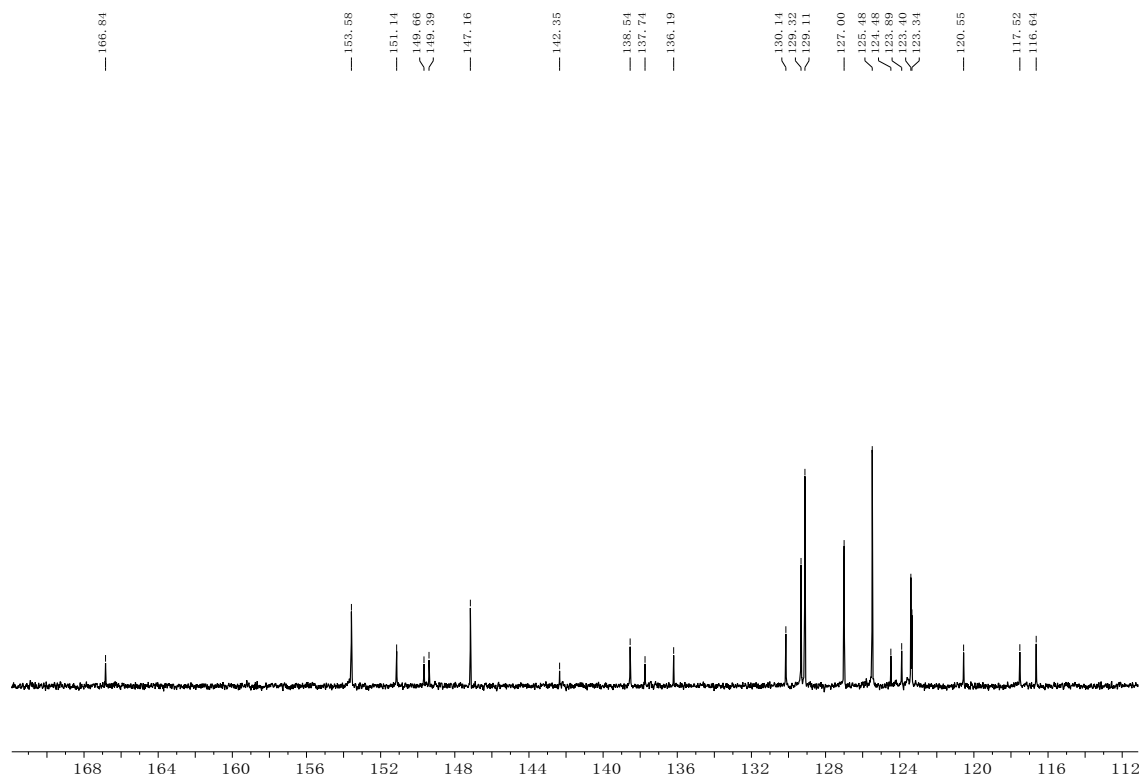
Under a nitrogen atmosphere, 4-(diphenylamino)phenylboronic acid (5.00 g, 0.02 mol), 2-bromopyridine (3.28 g, 0.02 mol) and Pd(PPh₃)₄ (1.00g, 0.86 mmol) were heated to 100 °C for 16 h in a mixed solvent of 2 M Na₂CO₃ and THF. After the reaction, the mixture was extracted with CH₂Cl₂ three times. The organic phase was dried over by anhydrous Na₂SO₄ and then purified by column chromatography, using petroleum ether as the eluent. The final product was white solid (4.40

g, 79%). ^1H NMR (400 MHz, CDCl_3): δ (ppm) 8.65 (d, $J = 4.4$ Hz, 1H), 7.86 (d, $J = 8.8$ Hz, 2H), 7.74–7.65 (m, 2H), 7.30–7.25 (m, 4H), 7.19–7.13 (m, 7 H), 7.05 (t, $J = 7.2$ Hz, 2H).

[(PAY)Pt(II)] μ -Cl $_2$ [(PAY)Pt(II)]



Under a nitrogen atmosphere, K_2PtCl_4 (5.00 g, 0.01 mol) and L-N (4.27 g, 0.01 mol) were heated to 90 °C for 16 h in a mixed solvent of 2-ethoxyethanol (22.5 mL) and water (7.5 mL). After cooling to the room temperature, saturated NaCl solution was added and the coarse dimer was collected by filtration and dried under vacuum.

Figure F.1 ¹H NMR spectrum of Pt-Ph-1Fig. S1 ¹H NMR spectrum and ¹³C NMR spectrum of Ph-PAYPt1

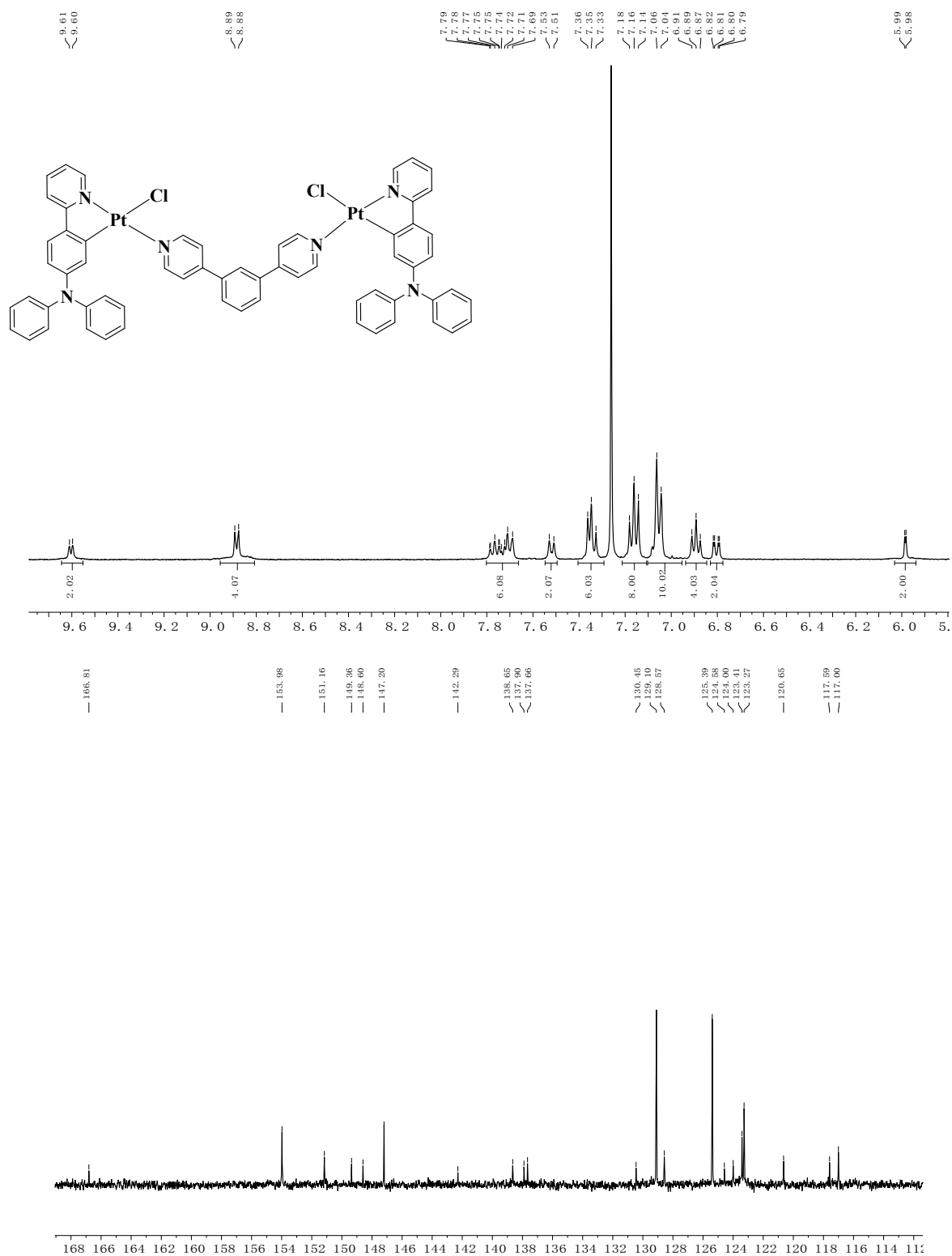


Fig. S2 ^1H NMR spectrum and ^{13}C NMR spectrum of Ph-PAYPt2

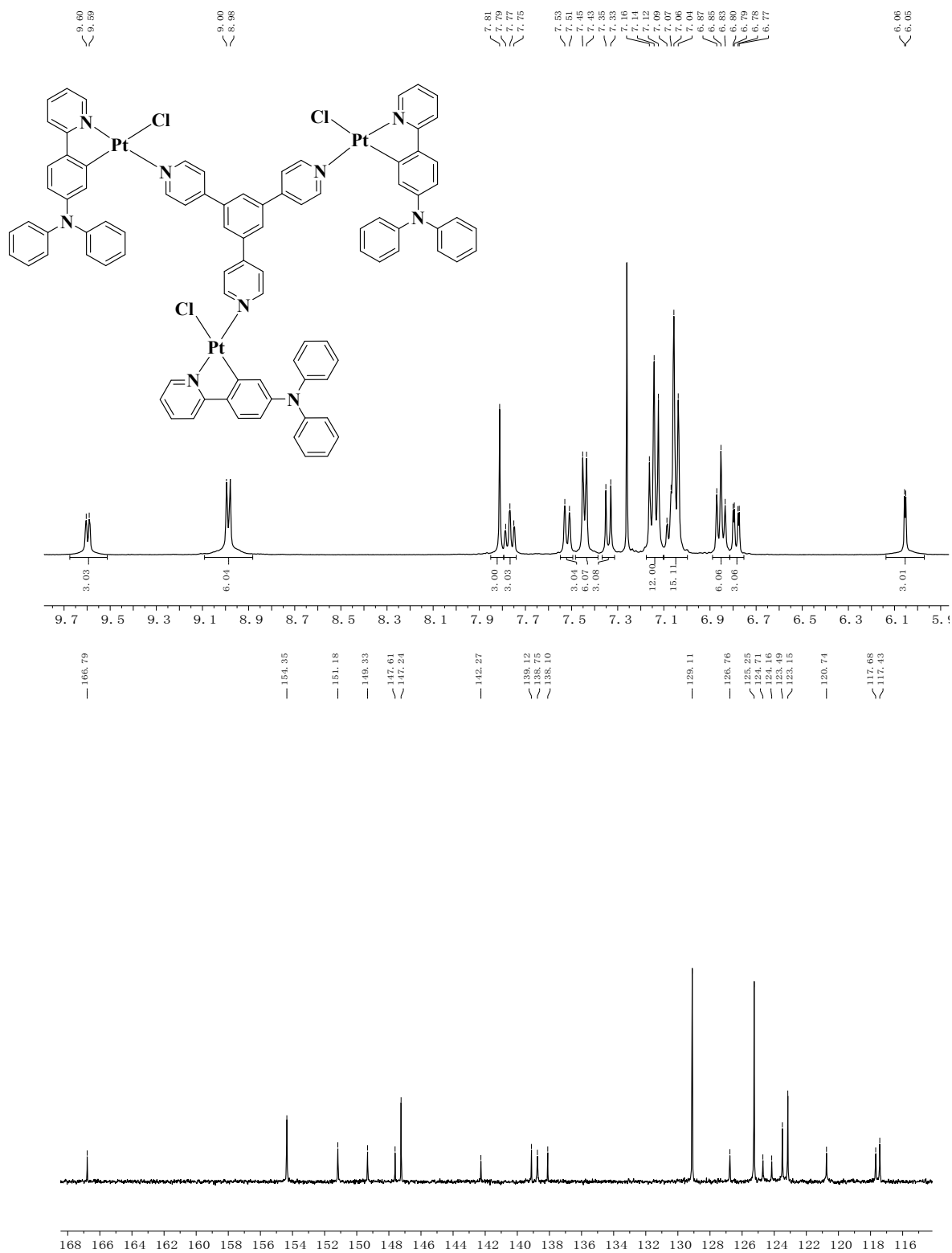


Fig. S3 ^1H NMR spectrum and ^{13}C NMR spectrum of Ph-PAYPt3

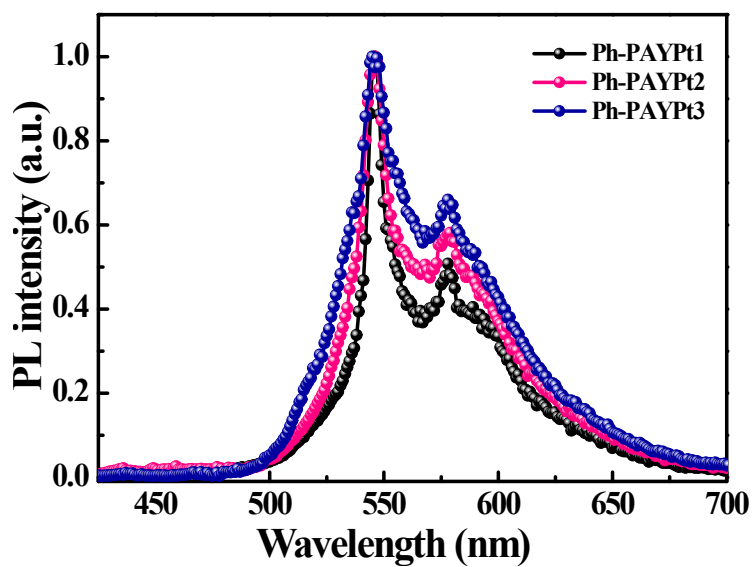


Fig. S4 PL spectra of these mono-, di- and tri-nuclear Pt^{II}(C[^]N)(N-donor ligand)Cl complexes in CH₂Cl₂ at 77 K.

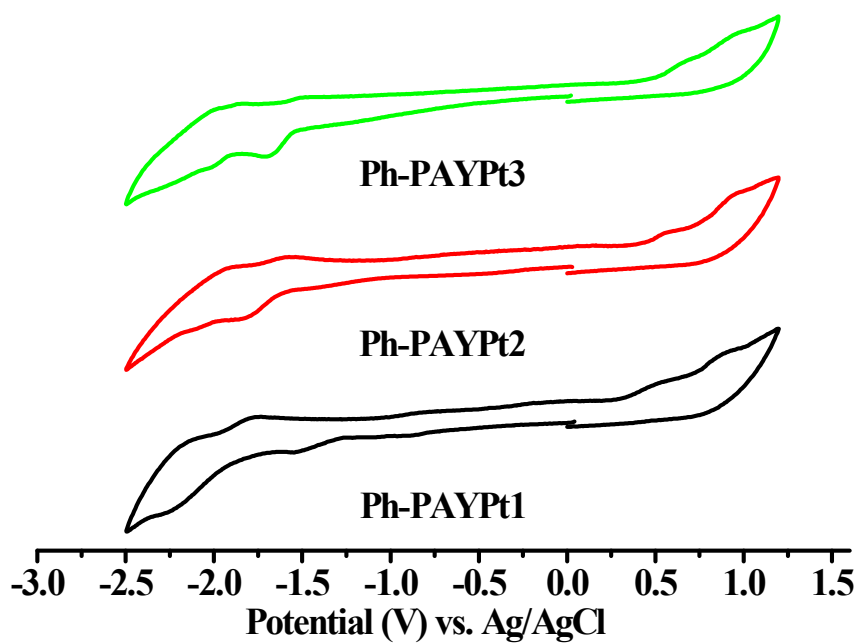


Fig. S5 CV curves for Ph-PAYPt1, PhPAYPt2 and PhPAYPt3

OLED fabrication and measurements

The ITO glass substrates were cleaned in advance and exposed to ultraviolet-ozone for *ca.* 7 min. The PEDOT:PSS, which plays the role of a hole injection layer, was spin-coated on the ITO glass substrates and then annealed at 120 °C for 20 min in the air. Then, the chlorobenzene solution containing the host materials and emitters with a certain doping ratio was spin-coated on surface of PEDOT:PSS layer to form the emission layer. The obtained ITO chip was dried at 80 °C for 20 min before it was transferred to the deposition system to deposit other active layers, i.e., electron-transporting layer, electron-injection layer and Al cathode. The orange phosphorescent Ir-Tz-1 was synthesized by our laboratory. The EL spectra and CIE coordinates were measured with a PR655 spectra colorimeter. The driving voltages and efficiencies of the devices were measured with the Keithley 2400/2000 source meter. The efficiency and spectral measurements were carried out under ambient conditions.

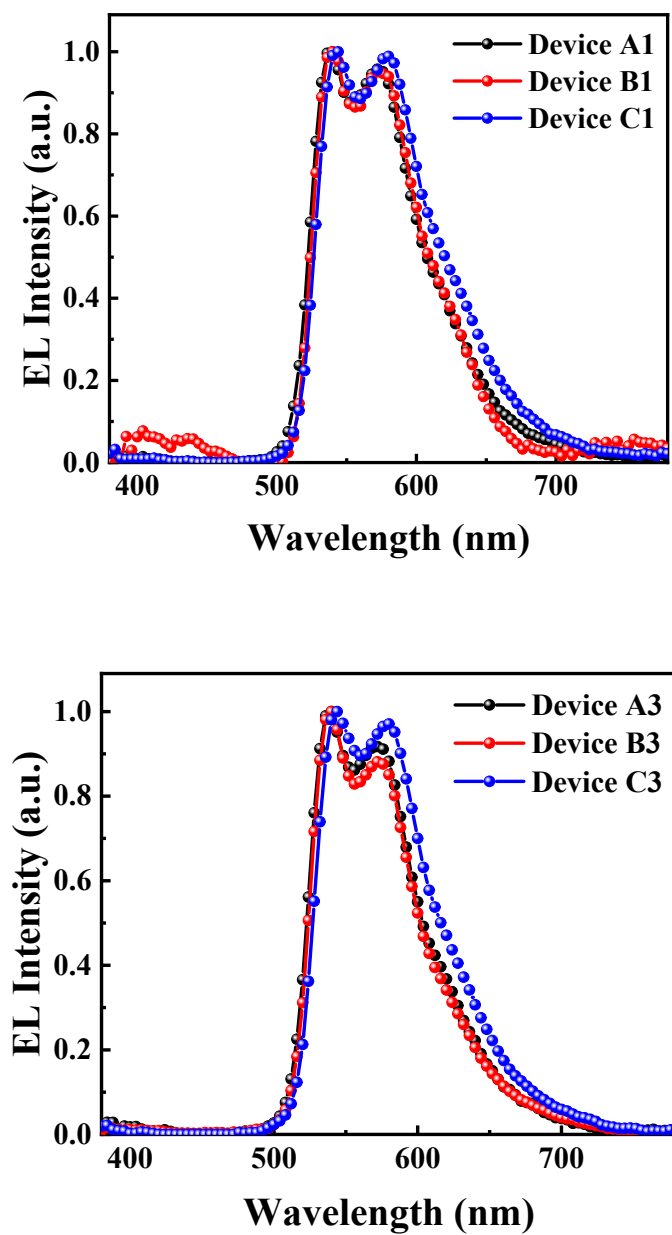


Fig. S6 EL spectrum for the devices except the optimized ones.

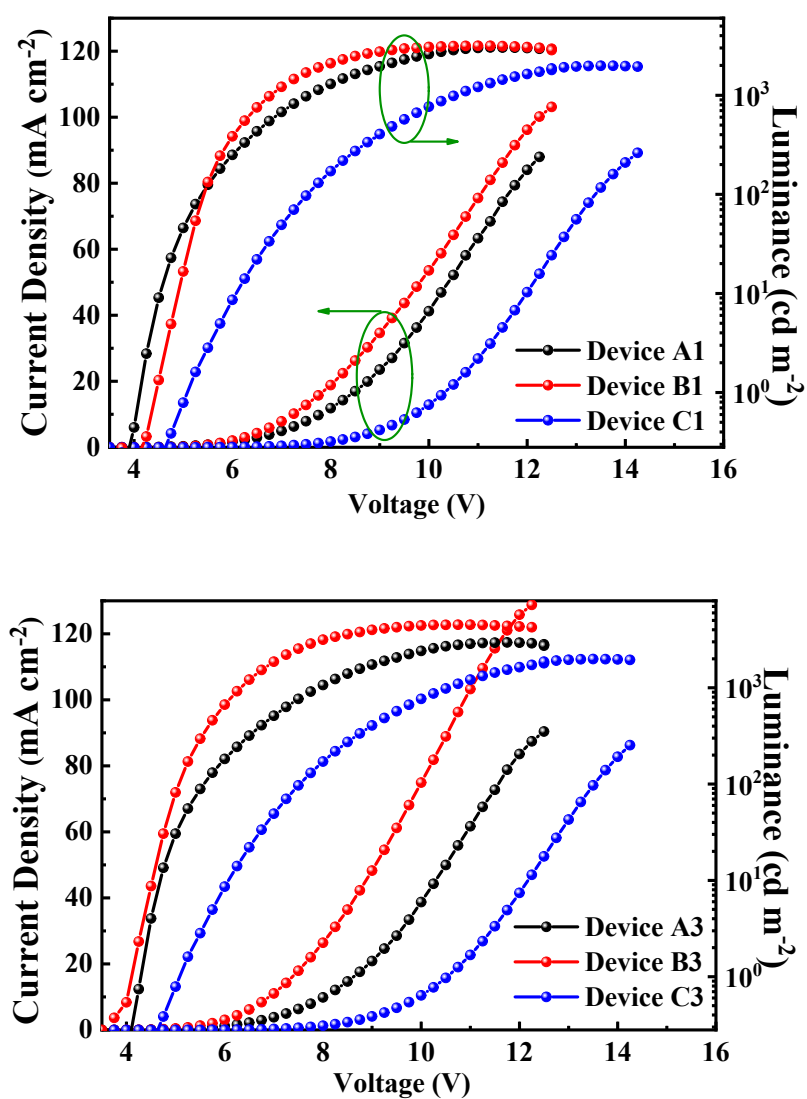


Fig. S7. Current density–voltage–luminance (J – V – L) curves for the devices except the optimized ones.

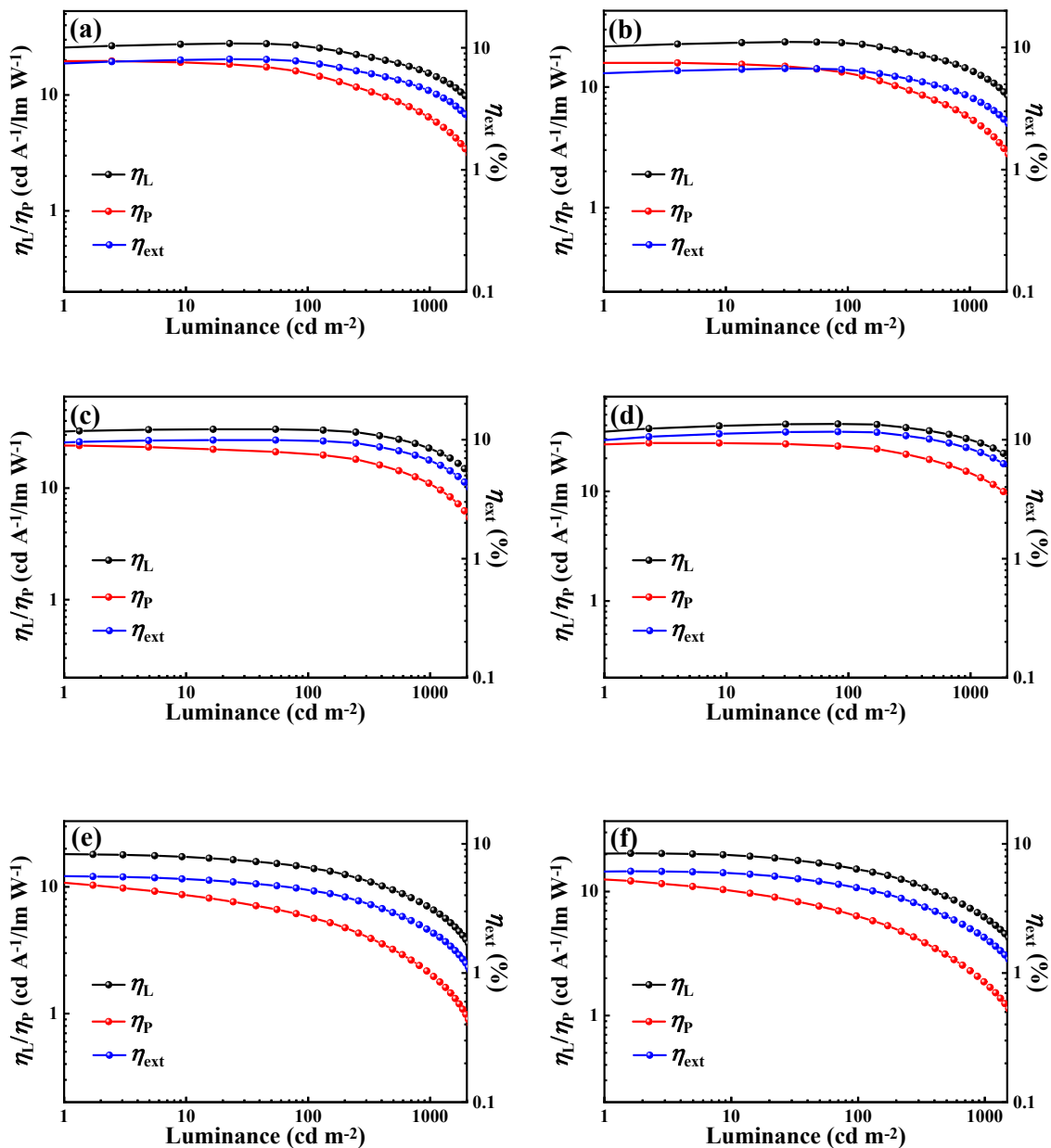


Fig. S8. Relationship between EL efficiencies and luminance for the devices except the optimized ones. (a) Device **A1**, (b) Device **A3**, (c) Device **B1**, (d) Device **B3**, (e) Device **C1** and (f) Device **C3**.